

Structure and Energetics of the Hydronium Hydration Shells

Omer Markovitch and Noam Agmon*

Department of Physical Chemistry and the Fritz Haber Research Center, The Hebrew University, Jerusalem 91904, Israel

Received: December 27, 2006; In Final Form: February 12, 2007

Proton solvation and proton mobility are both subjects of great interest in chemistry and biology. Here we have studied the hydration shells of H_3O^+ at temperatures ranging from 260 to 340 K using the multistate empirical valence-bond methodology (MS-EVB2). We have calculated the radial distribution functions for the protonium and its solvation shells. Furthermore, we have determined the Gibbs energy and the enthalpy for hydrogen bonds donated or accepted by the first two solvation shells, in comparison to bulk water. We find systematic bond-energy differences that appear to agree with a recent IR study on proton hydration. Implications of our results to various proton mobility mechanisms are discussed.

Introduction

Proton solvation and proton mobility are a subject of renewed interest.^{1,2} In bulk liquid water they are connected because the hydrogen-bond (HB) network solvating the hydronium (H_3O^+) is thought to determine the rate of proton mobility (PM). Thus far, most discussions of proton solvation in liquid water have concentrated on the two limiting structure, the “Eigen”³ (H_3O^+) and “Zundel”⁴ (H_5O_2^+) cations. However, Eigen has already anticipated that additional HBs participate in solvating the hydronium, which he has designated as H_9O_4^+ . The three water molecules coordinated to the H_3O^+ must therefore have extra-strong HBs. This type of HB is denoted by D0 in Figure 1: The “D” indicates that it is *donated* from the protonated center and the index i (here, $i = 0$) is the solvation shell from which it is donated. A linear correlation of HB strengths with HB lengths suggested that the strength of the D0 bond is 18.4 kJ/mol,⁵ as compared with 10.6 kJ/mol in bulk water, which was determined from Raman measurements.^{6,7} Yet, though molecular-dynamics (MD) simulations have been applied to determine the HB strength in bulk liquid water,⁸ no such simulations were performed for protonated water.

Does the hydronium affect only its first-shell neighbors, as anticipated by Eigen, or does its influence extend further into the bulk? There are currently contradictory experimental answers to this question. Transient near-IR measurements indicate that first shell water molecules around ions exhibit slower reorientation times than in the bulk, due to their stronger HBs with the central ion.⁹ However, this effect does not extend beyond the first shell. In contrast, a recent FTIR study of acids in HOD solutions exhibits, after eliminating the contributions from the bulk, discrete bands attributed to four hydration shells.¹⁰ Each of the donor HBs in Figure 1: D0, D1, D2, and sometimes D3 (not shown), is suggested to have its conjugate OD band at a different IR frequency.

Models of proton mobility in water are intimately connected with the surrounding HB pattern. Early on, Bernal and Fowler¹¹

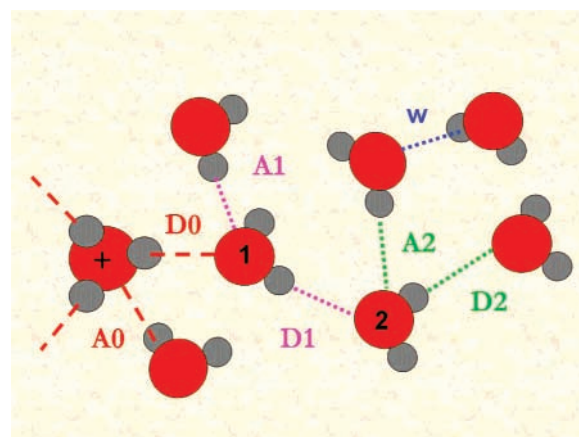


Figure 1. HB types discussed in this work with the layer color code used in all subsequent figures. D_i are bonds donated by the protonated center, and A_i are accepted by it. Oxygens are red, and hydrogens gray.

suggested that H_3O^+ migrates by proton hopping onto a water molecule rotating in its first solvation shell, requiring a broken D0 bond. This scenario is not plausible if indeed this HB energy is large as expected.^{12–14} Yet, there was no calculation performed to verify such a conclusion.

Recently, two novel scenarios for PM in liquid water were suggested, on the basis of either experimental data^{13,14} or ab initio MD simulations.^{15,16} These two models are best characterized as Eigen–Zundel–Eigen^{13,14,16} and Zundel–Zundel¹⁵ transformations (Supporting Information, Figure S1). In both models the postulated rate-limiting step was cleavage of a A1 type HB (defined in Figure 1). A1 cleavage was also suggested to occur in the initial stage of acid dissociation in liquid water.¹⁷ However, multistate empirical valence-bond (MS-EVB) simulations questioned this,^{18–20} because the average coordination number of the relevant first-shell oxygen appeared to change by less than a full unit. A recent analysis suggested that cleavage of D1 bonds on the donor side is at least as important as cleavage of A1 bonds on the acceptor side.²¹ Yet there has been no

* Corresponding author. E-mail: agmon@fh.huji.ac.il.

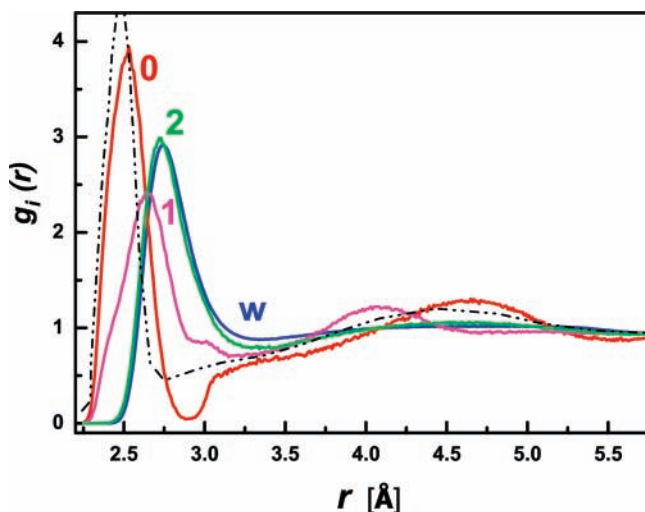


Figure 2. Comparison of oxygen–oxygen radial distribution functions centered on the hydronium, its first- and second-shell water ligand, with that of pure water according to our MS-EVB2 simulations at $T = 300$ K. The area under the water peak corresponds to 4.5 neighbors, in comparison with 4.35 from TIP3P water simulations (Table II of ref 26). The black dash-dot curve is $g_0(r)$ from a neutron scattering experiment from concentrated HCl (Figure 6 of ref 23). The too-deep depression in the calculated $g_0(r)$ around 2.9 Å reflects an inadequate MS-EVB2 parameter.

quantitative assessment of the relevant HB strengths to validate these claims.

To address these questions concerning proton solvation and proton mobility, we have utilized MD simulations based on the MS-EVB methodology of Schmitt and Voth²² to investigate the HB enthalpies and entropies for the hydronium solvation shells in liquid water.

Method

We have run second-generation MS-EVB²⁰ trajectories for 216 water molecules plus a single proton in a 18.64 Å-wide cube (corresponding to a density $\rho = 1.0$ g/cm³ at 300 K) with periodic boundary conditions and Ewald summation, at several temperatures (T) between 260 and 340 K. Each trajectory was first equilibrated (NVT ensemble) for about 100 ps and then run (with 0.5 fs time steps) without the thermostat (NVE ensemble) for 250 ps, saving the atomic coordinates every 25 fs. At each temperature several (3–10) such trajectories were generated (with different initial conditions), producing up to 100 000 time frames constituting the sample space for the statistics reported below. For each frame, the hydronium oxygen was identified as the one with the three closest hydrogen atoms, and its first two solvation shells were constructed by a nearest-neighbor search algorithm (see Figure 1). Water molecules not forming HBs to these shells were defined as “bulk water”.

Results

Figure 2 shows the radial O–O distribution functions at 300 K, with the origin on the H_3O^+ oxygen atom ($g_0(r)$), on a first-shell ($g_1(r)$), second-shell ($g_2(r)$), or bulk ($g_w(r)$) water oxygen. The first peak in $g_0(r)$ is sharp and centered around 2.53 Å. This is in close agreement with experimental data for concentrated HCl,²³ whose first peak is at 2.48 Å (black dash-dot line). The chloride ion may be responsible for the somewhat narrower experimental peak. For $g_1(r)$, it is shifted to larger r and is wider (hence, lower). This reflects contributions from two kinds of HBs: a single D0 bond with H_3O^+ , vs several D1 and A1 HBs.

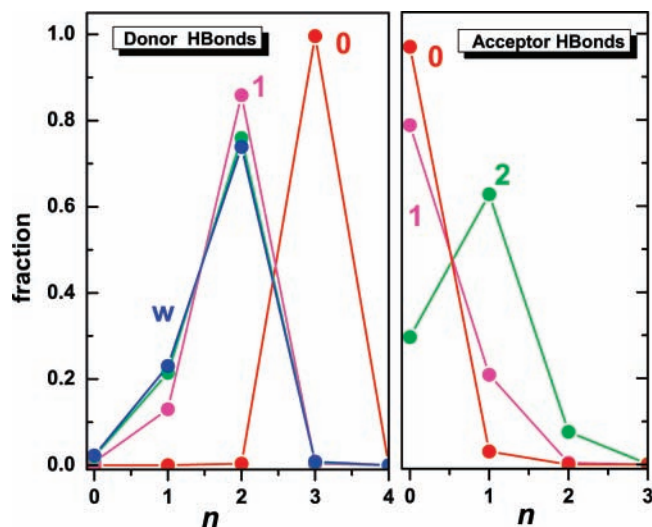


Figure 3. Probability distributions for the number of HBs for each of the five types of HBs in Figure 1 at $T = 300$ K. For water we consider only the donor bonds.

$g_2(r)$ is already close to $g_w(r)$, with peaks at 2.73 and 2.75 Å, respectively. This seems to support the observation of Omta et al.⁹ that the enhanced order induced by an ion extends only to the first solvation layer. The population under the first peak, $4\pi\rho\int_0^{R_{\min}} g_i(r)r^2 dr$, is 3.0 and 2.9 for $i = 0$ and 1, respectively ($R_{\min} = 3.0$ Å). The coordination number of the hydronium and its first solvation shell is close to 3 because, as we shall see below, A0 and A1 are extremely weak HBs.

To proceed with HB strength calculations, one must first define a HB. There are several alternatives.²⁴ For simplicity, we have utilized here the conventional geometrical criterion requiring an O–O distance smaller than a certain cutoff (R_{OO}) and an $\text{O}\cdots\text{OH}$ angle smaller than 30° (Figure S2). One might think that R_{OO} should be taken as R_{\min} , the first minimum in $g(r)$. We find that the thermodynamic properties calculated below are sensitive to the cutoff value near the minimum in $g(r)$. The results are converged if a larger R_{OO} is taken, as demonstrated in Figure S3 of the Supporting Information.

Figure 3 depicts the distributions, $p(n)$, of the number of HBs per water molecule, n , for the different types defined in Figure 1. Note that we have not separated “Zundel” (H_5O_2^+) from the “Eigen” (H_3O^+) cations. For D0 the most probable n (denoted n^*) is 3, and for D1 and D2 $n^* = 2$, corresponding to a single HB per hydrogen. Cases with one broken or one bifurcated HB correspond to $n = n^* - 1$ and $n^* + 1$, respectively. The probability of having two bifurcated or two broken HBs on the same water molecule is practically zero. The distribution of D2 bonds is almost identical to that of the donor bonds of pure water, but for D1 it is narrower, with smaller $p(n^* - 1)$ indicating a stronger HB. For acceptor-type HBs, A_i , we expect a distribution peaking at $n^* = 1$ because we do not count the HB emanating from the protonated center. This holds for A2 bonds, but for A0 and A1 we find $n^* = 0$, indicating that this HB is usually broken.

From each distribution we define an equilibrium constant, K_{eq} , for HB cleavage (bonded \rightleftharpoons nonbonded reaction)

$$K_{\text{eq}} = p(n < n^*)/p(n^*) \quad (1)$$

Note that we count the number of HBs for a hydrogen atom pair in a given water molecule (and not for each H separately). This parallels the analysis of the Raman spectrum of liquid water, where the OH stretch band is decomposed into contribu-

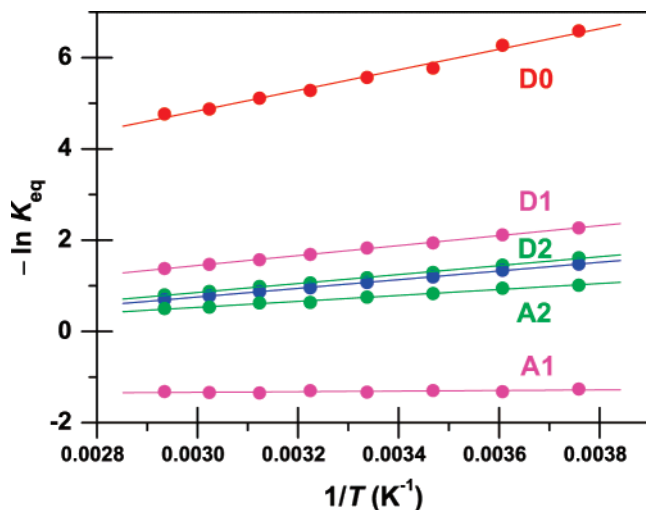


Figure 4. van't-Hoff plot for the equilibrium constant for HB cleavage, eq 1, as a function of inverse temperature. The HB strengths, ΔH^0 , are extracted from the linear fits (correlation coefficients square ≥ 0.99 , except for A1 where a poor linear fit is achieved) and collected in Table 1. Refer to Figure 1 for HB type definition.

TABLE 1: Thermodynamic Parameters (kJ/mol) for Hydrogen Bonds in the Hydronium Solvation Shells from MS-EVB2 Simulations of Protonated Water at 300 K (Extracted from the Linear Fits in Figure 4)

HB type	ΔG^0	$T\Delta S^0$	ΔH^0
D0	13.8	4.5	18.3
D1	4.6	4.5	9.1
D2	2.9	5.2	8.1
water	2.7	5.2	7.9
A2	1.9	3.5	5.4
A1	-3.3	3.9	0.6

tions from bonded vs nonbonded species, as evidenced by an isosbestic point.⁶ Similar (though not identical) definitions were applied in simulations⁸ and models²⁵ of liquid water. Given the ergodic hypothesis, that time averages converge to ensemble averages, we treat K_{eq} as a true thermodynamic quantity, so that the standard Gibbs energy of HB cleavage is given by $\Delta G^0 = -RT \ln K_{eq}$ (the standard state here is $\rho = 1.0 \text{ g/cm}^3$). Figure 4 shows linear van't Hoff plots of $-\ln K_{eq}$ vs $1/T$. Their slopes equal to $\Delta H^0/R$, where ΔH^0 is the HB strength and R is the gas constant. The standard entropy for HB dissociation is obtained from $\Delta G^0 = \Delta H^0 - T\Delta S^0$, and all the values are collected in Table 1.

Discussion

In bulk water all the HBs are on average equivalent, with $\Delta H^0 = 7.9 \text{ kJ/mol}$. This is close to 7.0 kJ/mol for TIP3P water,⁸ the underlying water model of MS-EVB2²⁰ (but somewhat smaller than the experimental value of 11 kJ/mol). Part of the difference between the two calculations is because we counted only HBs donated by the two hydrogens of each water molecule, which can be more easily compared with the hydronium solvation shells. The D2 bond enthalpy is nearly equal to that of bulk water, whereas the A2 bond is somewhat weaker. The effect is enhanced as the hydronium is approached ($i = 2, 1$, and 0): the D_i bonds strengthen whereas the A_i bonds weaken. The reason for this²¹ is the charge delocalization in the MS-EVB2 potential:²⁰ the H_3O^+ carries on average 65% of the charge, and ca. 11% is delocalized on each of its three water ligands. A water molecule would preferentially point one of its oxygen lone pairs toward a positive center, and not one of its

protons. In contrast, $T\Delta S^0$ is nearly constant (ca. 5 kJ/mol) for all D_i bonds, and somewhat smaller ($\approx 3.5 \text{ kJ/mol}$) for the A_i bonds.

D0 is indeed the strongest HB in protonated water. Its calculated bond enthalpy, cited in Table 1, is (fortuitously) close to the value of 18.4 kJ/mol previously suggested from a linear bond-energy/bond-length correlation.⁵ This supports Eigen's vision³ that the hydronium is better described as a larger cation, H_9O_4^+ , which includes H_3O^+ with its first solvation shell. A consequence of the increased effective radius is that the non-Grotthuss component of proton mobility must be *smaller* than water self-diffusion.⁵ A "rigid sphere" picture of the Eigen cation could also enhance the viscosity of concentrated acids according to the Einstein model.⁹

In this study we find *two* solvent layers that differ from the bulk, with unique values for the D0, D1, A0, A1, and A2 HBs. The $g(r)$ of the second solvation shell looks similar to that for bulk water, yet it accepts one strong (D1) and one weak (A2) HB. Thus it is not yet completely bulk-like. This may be characteristic of the delocalized hydronium, as opposed to other cations for which only the first-shell differs from the bulk.⁹

At first our conclusion seems at odds with the results of ref 10, but this is only because the five IR peaks in Figure 9 there were arbitrarily assigned to D0, D1, D2, D3, and D4 (in the order of increasing frequency). They could be assigned differently, for example to the D0, D1, A2, A1, and A0 bonds, respectively. From Table 1 we find that $\Delta\Delta H^0$ is 9.2 kJ/mol for D0 minus D1, and 3.7 kJ/mol for D1 minus A2. The corresponding energetic differences between the first three peaks there¹⁰ (multiplied by $\sqrt{2}$ to correct for the isotope effect) are 8.4 and 3.6 kJ/mol , respectively. This is a remarkable agreement. However, the A2 minus A1 difference is 4.8 kJ/mol , whereas experimentally it is 1.8 kJ/mol . This suggests that the A1 HB strength might be larger than that found from the present potential, ca. 3.5 kJ/mol .

Returning to the mechanism of proton mobility, its activation energy for the MS-EVB2 potential is $E_A = 11.3 \text{ kJ/mol}$; see Figure 2 in ref 21. The D0 bonds are considerably stronger than this and thus cannot break during PM as suggested by Bernal and Fowler.¹¹ For the A1 bonds ΔH^0 is at most 3.5 kJ/mol (see above), and hence the cleavage of a *single* A1 bond cannot comprise the rate-limiting step, as previously assumed.^{13,15} In contrast, for D1 we find $\Delta H^0 \approx E_A$, so for the present potential their cleavage could be part of the rate-limiting step, possibly together with collective effects.²¹

Finally, one may ask whether MS-EVB2 is sufficiently accurate to distinguish between the different types of HBs portrayed in this work. This is tantamount to asking whether it can successfully discriminate between the various scenarios suggested for proton mobility. To answer these questions, simulations are underway for additional protonated water potentials.

Acknowledgment. We are indebted to Gregory A. Voth and Matt K. Peterson for discussions and instructions in using MS-EVB2. This research was supported by the Israel Science Foundation (grant number 191/03). The Fritz Haber Research Center is supported by the Minerva Gesellschaft für die Forschung, GmbH, München, FRG.

Supporting Information Available: Text and figures describing PM mechanisms, cutoff definitions, and the criterion used for HBs (PDF). This material is available free of charge via the Internet at <http://pubs.acs.org>.

References and Notes

- (1) Special Issue on Proton Solvation and Proton Mobility. Agmon, N., Gutman, M., Eds. *Isr. J. Chem.* **1999**, *39* (3/4).
- (2) Voth, G. A. *Acc. Chem. Res.* **2006**, *39*, 143–150.
- (3) Eigen, M.; Kruse, W.; Maass, G.; De Maeyer, L. *Prog. React. Kinet.* **1964**, *2*, 287–318.
- (4) Zundel, G. Easily Polarizable Hydrogen Bonds – Their Interactions with the Environment – IR Continuum and Anomalous Large Proton Conductivity. In *The Hydrogen Bond, Recent Developments in Theory and Experiments*; Schuster, P., Zundel, G., Sandorfy, C., Eds.; North Holland: Amsterdam, 1976; Chapter 15, pp 687–766.
- (5) Agmon, N. *J. Chim. Phys. Phys.-Chim. Biol.* **1996**, *93*, 1714–1736.
- (6) Walrafen, G. E.; Fisher, M. R.; Hokmabadi, M. S.; Yang, W.-H. *J. Chem. Phys.* **1986**, *85*, 6970–6982.
- (7) Carey, D. M.; Korenowski, G. M. *J. Chem. Phys.* **1997**, *108*, 2669–2675.
- (8) van der Spoel, D.; van Maaren, P. J.; Larsson, P.; Timneanu, N. *J. Phys. Chem. B* **2006**, *110*, 4393–4398.
- (9) Omta, A. W.; Kropman, M. F.; Woutersen, S.; Bakker, H. J. *Science* **2003**, *301*, 347–349.
- (10) Śmiechowski, M.; Stangret, J. *J. Chem. Phys.* **2006**, *125*, 204508.
- (11) Bernal, J. D.; Fowler, R. H. *J. Chem. Phys.* **1933**, *1*, 515–548.
- (12) Agmon, N.; Goldberg, S. Y.; Huppert, D. *J. Mol. Liq.* **1995**, *64*, 161–195.
- (13) Agmon, N. *Chem. Phys. Lett.* **1995**, *244*, 456–462.
- (14) Agmon, N. *Isr. J. Chem.* **1999**, *39*, 493–502.
- (15) Tuckerman, M.; Laasonen, K.; Sprik, M.; Parrinello, M. *J. Phys. Chem.* **1995**, *99*, 5749.
- (16) Marx, D.; Tuckerman, M. E.; Hutter, J.; Parrinello, M. *Nature* **1999**, *397*, 601–604.
- (17) Ando, K.; Hynes, J. T. *J. Mol. Liq.* **1995**, *64*, 25–37.
- (18) Vuilleumier, R.; Borgis, D. *Isr. J. Chem.* **1999**, *39*, 457–467.
- (19) Day, T. J. F.; Schmitt, U. W.; Voth, G. A. *J. Am. Chem. Soc.* **2000**, *122*, 12027–12028.
- (20) Day, T. J. F.; Soudackov, A. V.; Čuma, M.; Schmitt, U. W.; Voth, G. A. *J. Chem. Phys.* **2002**, *117*, 5839–5849.
- (21) Lapid, H.; Agmon, N.; Petersen, M. K.; Voth, G. A. *J. Chem. Phys.* **2005**, *122*, 014506.
- (22) Schmitt, U. W.; Voth, G. A. *J. Chem. Phys.* **1999**, *111*, 9361–9381.
- (23) Botti, A.; Bruni, F.; Imberti, S.; Ricci, M. A.; Soper, A. K. *J. Chem. Phys.* **2004**, *121*, 7840–7848.
- (24) Luzar, A. *J. Chem. Phys.* **2000**, *113*, 10663–10675.
- (25) Silverstein, K. A. T.; Haymet, A. D. J.; Dill, K. A. *J. Am. Chem. Soc.* **2000**, *122*, 8037–8041.
- (26) Wu, Y.; Tepper, H. L.; Voth, G. A. *J. Chem. Phys.* **2006**, *124*, 024503.